ACADEMIA ROMÂNĂ
Revue Roumaine de Chimie
https://www.icf.ro/rrch/

Rev. Roum. Chim.,
2026, *71*(3–4), 225–243
DOI: 10.33224/rrch.2026.71.3-4.07

IMPROVING THE HYDROLYSIS BEHAVIOR OF IMINE-LINKED GRAFT MONOMER AND COPOLYMER CARRIERS FOR CONTROLLED RELEASE: A KINETIC STUDY OF COPOLYMER COMPOSITION AND pH EFFECT

Meryem MOUFFOK,[*,a,b,c] Awatif Amaria MOULAY,[b]
Ilham ABDELMALEK[d], and Abderrezzak MESLI[b]

[a] Laboratory of Elaboration and Characterization of Materials (LECM), Djillali Liabes University, Sidi Bel-Abbes 22000, Algeria
[b] Laboratory of Macromolecular Physical and Organic Chemistry, University of Djillali Liabes, Sidi Bel-Abbes 22000, Algeria
[c] Department of Electronics, Faculty of Electrical Engineering, Djillali Liabes University, Sidi-Bel-Abbes 22000, Algeria
[d] Synthesis and Catalysis Laboratory, University of Ibn Khaldoun, Tiaret 14000, Algeria

Received August 9, 2025

The current work investigates the hydrolysis behavior of synthesized Schiff's base, N-vinylbenzylidene-*p*-anisidine, and its copolymers (Cp_1, Cp_2) with *N*,*N*-dimethylacrylamide in acidic (pH 1.2) and basic (pH 8) heterogeneous media at 37 °C using UV-Vis spectroscopy. The effects of polymer molecular weight and pH on drug release constants were evaluated. A comparative study was carried out between homogeneous and heterogeneous media at different pH values to elucidate the hydrolysis kinetics process of the imine function, and to identify the optimal medium for achieving a sustained-release profile. The kinetics data indicated that hydrolysis of the imine function in homogeneous conditions follows first-order kinetics, whereas in heterogeneous media the process is governed by Fickian diffusion. The hydrolysis rate was found to increase with acidity and is influenced by both pH and polymeric carrier. The results demonstrated that the molecular weight of the polymers significantly influences both the drug release constants and the diffusion mechanism. Higuchi's model confirmed that drug release in heterogeneous media is slower and more prolonged, where the amounts of *p*-AN released are not only lower but also occur over extended intervals.

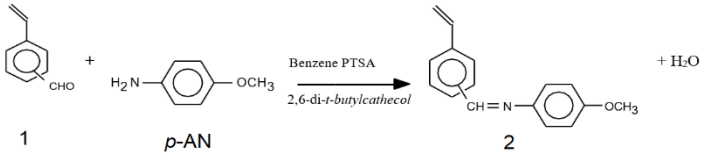

1 *p*-AN 2

INTRODUCTION

The use of natural or synthetic macromolecular structures as carriers or excipients in the drug delivery systems has been the focus of substantial research activity and development over the past decade, owing to their diverse therapeutic applications.[1–4] As demonstrated by Rana *et al.*,[2] smart polymeric micelles provide tunable and stimuli-responsive release kinetics, thereby allowing precise control over the timing and rate of drug release. Specifically, modifying polymer properties—such as composition, molecular weight, and hydrophilic – lipophilic balance – directly influences drug solubility, matrix swelling, and diffusion dynamics, thereby enhancing bioavailability and enabling targeted release.[4] These carriers protect the drug during transit through hostile environments (gastric acid), ensuring its controlled delivery at the intended site.[1–3] The

* Corresponding author: m.mouffok@univ-chlef.dz, https://orcid.org/0000-0003-4306-5368

overall goal is to optimize the pharmacokinetic profile for sustained therapeutic efficacy. Bio-active polymers are typically classified into two categories: (i) polymers exhibiting intrinsic therapeutic activity; and (ii) biologically inert carriers designed for drug delivery systems.[3,4]

Our study focuses on the last category, where the active agent is covalently grafted to the polymeric carrier through a via a hydrolyzable azomethine (>C=N–) linkage, enabling release under gastrointestinal conditions. Recent advances have been noted in the chemical grafting of active agents onto polymer chains to control drug release rate, where drugs are either dispersed within or chemically bound to the polymer backbone.[2–4] The mechanism of imine hydrolysis has long been a subject of foundational research by Hammett,[5] Jencks,[6,7] and Layer.[8] In particular, the hydrolysis behavior of Schiff bases has drawn attention due to its relevance in designing pH-sensitive hydrolysis, allowing effective delivery of amine-containing drugs with controlled release.[7–9]

The first kinetic studies by Kamogawa *et al.*,[9] established that mono-imines hydrolyze more rapidly than polymeric derivatives in homogeneous media. Complementary work by Huang *et al.*[10] in heterogeneous systems showed the strong influence of solvent polarity on hydrolysis rate. These foundational studies have substantially advanced our understanding of Schiff base hydrolysis mechanisms. Notably, Mesli *et al.* investigated the hydrolysis kinetics of pyrrolic aldehyde–derived Schiff bases in buffered ethanol and sulfuric acid solutions, highlighting the structural effects of substituents on reaction rates.[11–19] More recently, Mesli and Liu extended these findings by systematically exploring mechanism insights of substituent effects on Schiff base hydrolysis and computational modelling.[18–20] Schiff' bases undergo hydrolysis more readily than their polymeric counterparts;[21–24] these findings align with our previous experimental observations and provide a strong rationale for further exploring hydrolysis behavior under heterogeneous conditions. Imine compounds play a pivotal role across in diverse fields, ranging from medicinal and biological chemistry,[25] to applications in protein-based hydrogels,[26] corrosion inhibition,[27] and drug delivery systems involving grafted active molecules.[21–24,28]

Despite this extensive literature, this study aims to provide additional insights data related to the behavior of imine-containing systems under heterogeneous conditions. *p*-Anisidine (*p*-AN), is also known as a Δ6 desaturation inhibitor in *Mortierella alpina* strains.[29] In this work, *p*-AN is grafted on (*m,p*)-Vinylbenzaldehyde (VBA) monomer and copolymers through imine link for controlled release. (*m,p*)-VBA was selected for its dual functionality: a polymerizable ethylenic group substituted with a "spacer phenyl group", bearing an aldehyde functionality which allowed the imine linkage between the amine and the polymer backbone. Although, N,N-dimethylacrylamide (DMA) assure pH-independent sustained release. So, in our prior researches,[1,21] N-(*m,p*)-vinylbenzylidene-*p*-anisidine was synthesized and copolymerized with DMA at two molecular ratios, where the hydrolysis of imine function was studied in homogeneous media (pH 4–10),[1] and only in acidic heterogeneous media (pH 4–4.7).[21] The results showed that the imine function hydrolysis is extremely dependent on its carrier and the pH medium. Hence, the current study expands on this by modulating the drug release using these formulations in heterogeneous media, given that release kinetics following Schiff base hydrolysis is diffusion-controlled. Subsequently, the comparative study was performed between homogeneous and heterogeneous media at two pH levels corresponding to gastric (pH 1.2) and intestinal (pH 8.0) media at 37 °C using UV-Vis.

This work aims to investigate the hydrolysis mechanism of imine in heterogeneous media at different pH conditions in one hand, and in the other hand, to determine the effect of copolymerization composition on the hydrolysis constant in the two studied media. By using different carriers – namely the imine monomer and its copolymers – and the appropriate study media, the drug release through imine hydrolysis can be modulated and controlled over time.

MATERIALS AND METHODS

Materials

The selected commercial *p*-Anisidine (≥ 99%) and a mixture of (*m,p*)-*chloromethylstyrene* isomers in a 70/30% ratio (*m,p*-vinylbenzyl chloride, ≥ 98%, stabilized with tert-butylcatechol) were purchased from Sigma-Aldrich (Germany). The *N,N*-Dimethylacrylamide (≥ 99%) used in this study was a commercial product from Merck (Darmstadt, Germany). Hexamethylenetetramine

(HMTA, ≥ 99%), was purchased from Sigma-Aldrich (Germany) and Glacial acetic acid (≥ 99.7%) was purchased from Merck, Germany). 2,6-di-tert-butylcatechol (DTBC, ≥ 99%, Sigma-Aldrich, Merck, Germany) was used as an antioxidant and polymerization inhibitor. Sodium carbonate (Na_2CO_3, anhydrous, (≥ 99.5%) and Hydrochloric acid. (HCl, 37%, analytical grade) purchased from Merck, Germany were used without further purification.

Methods and Characterization of Schiff's Base and its copolymers

IR spectra were registered recorded using a FTIR-8300 Shimadzu spectrophotometer with samples dispersed in KBr pellets at the Measurement Center of the Faculty of Sciences (CMFS), University of

Djillali Liabes, Sidi-Bel-Abbes. The ^1H and ^{13}C NMR spectra of synthesized monomer and Schiff's base dissolved in deuterated DMSO-d6 at 25 °C were recorded on Brucker DRX 400 MHZ at the University of Science and Technology of Languedoc (USTL), Montpellier, France. The molecular weights of the copolymers were determined by GPC using a KNAUER system equipped with a set of ultra-styragel columns (10^3, 10^4, and 10^5 Å) with tetrahydrofuran (THF) as the eluent at a flow rate of 9.1 mL/min. Calibration was performed with polystyrene standards of known molecular weights at the Central Analytical Service of the CNRS in Solaize, France. Elemental microanalyses were carried out at the Central Analytical Service of the CNRS in Solaize, France. The melting point of the monomer was measured on a calibrated KÖFLER heating stage. Differential scanning calorimetry (DSC) thermograms were recorded on a Setaram DSC instrument (6 mg of copolymer, 5 °C/min) at the University Jean Monnet of Saint-Étienne, France. The kinetic study of the hydrolysis was monitored using a SHIMADZU UV-Vis 2401PC spectrophotometer at CMFS, University of Djillali Liabes, Sidi-Bel-Abbes, equipped with a thermostated cell compartment. The UV-Vis spectrum (200– 400 nm) of each imine in an absolute ethanol solution at $C = 10^{-4}$ mol L^{-1} was carried out using a UV-Vis Shimadzu UV-2401 PC; it presented four bands (λ_{max} in nm, ε in L cm^{-1} mol^{-1}).

Preparation and characterization of monomer carriers and copolymers

Synthesis of (m,p)-vinylbenzaldehyde 1

The monomer (*m,p*)-vinylbenzaldehyde (yellow oil) was synthesized according to Sommelet method described in our previous research[21] from the *(m,p)*-chloromethyl-styrene (CMS) (Scheme 1). 0.4 mol (60.8 g) of (*m,p*)-chloromethylstyrene ((*m,p*)-CMS), were placed in a 500 mL two-necked round-bottom flask equipped with a condenser, to which 0.4 mol (56.07 g) of hexamethylenetetramine (HMTA) was added. Then, 125 mL of glacial acetic acid, 125 mL of distilled water, and a few traces of 2,6-di-tert-butylcatechol (as a polymerization inhibitor) were added to the mixture. The reaction mixture was maintained at reflux at 100 °C for 2 h under vigorous stirring. Subsequently, 100 mL of concentrated hydrochloric acid (HCl) were added, and reflux was continued for an additional 15 min. After cooling, the yellowish-green product was extracted with ether. The obtained organic phase was washed several times with a 10% aqueous Na_2CO_3 solution and with distilled water until neutral pH (~7) was reached. The solution was dried over anhydrous sodium sulfate to remove traces of water and then concentrated under reduced pressure using a rotary evaporator. The final product was distilled under a pressure of 1 mmHg at 65 °C.

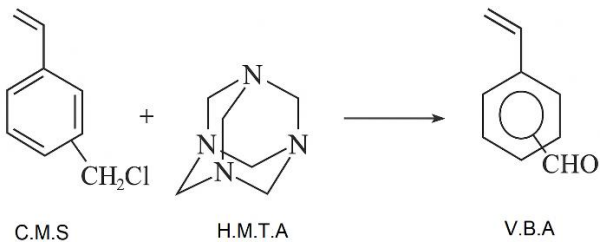

Scheme 1 – Synthesis of (*m,p*)-vinylbenzaldehyde (1).

Yield: 60%, IR (film on NaCl pellets) *t* (cm^{-1}): 1700.91 (C,O), 2732.64 and 2826.2 (HAC,O), 1609.5 (C,C), 1839.76 (,CH_2, overtone), 988.33 (,CAH), 917.95 (,CH_2),

3008.41 and 840.81 (ØAH); UV (Ethanol) k_1 max (e max) = 281 nm (20098), k_2 max (e max) = 218 nm (8987), k_3 max (e max) = 204 nm (12426); ^{1}H NMR (400 MHz, DMSO-d_6) d (ppm):10(s, H_1), 7.9 (d, H_2 and H_2';J = 8.19 Hz), 7.71 (d, H_3 and H_3', J = 8.15 Hz), 6.85 (dd, H_4, J = 17.64 Hz, J = 10.96 Hz), 6.06(d, H_6, J = 17.5 Hz), 5.48 (d, H_5, J = 10.96 Hz).

***Synthesis of the imine monomer carrier: N-(m,p)-vinylbenzylidene-p-anisidine (Im)* (2)**

The Schiff's base monomer derived from heterocyclic amine, N-(*m,p*)-vinylbenzylidene-*p*-anisidine (Im) and its copolymers with *N,N*-dimethylacrylamide Cp_1 and Cp_2 (Scheme 2 and 3) were synthesized according to the experimental procedure described in our prior research.[21] The compound (2) was obtained using the general reaction of Schiff's base synthesis presented in Scheme 2. An equimolar mixture of (*m,p*)-Vinylbenzaldehyde ((*m,p*)-VBA) and *p*-anisidine (*p*-AN) was heated under a Dean–Stark apparatus in benzene as the solvent, in the presence of traces of 2,4-di-tert-butylcatechol as an antioxidant and *p*-toluene sulfonic acid (PTSA) as the catalyst. The reaction was stopped upon recovery of the theoretical amount of water. After cooling, the solvent was removed using a rotary evaporator, and the residue was recrystallized several times from absolute ethanol. A yellow powder imine was collected giving 57% of yield.

Melting point mp = 47 °C was detected (Tottoli Büchi 510 apparatus); IR spectroscopy (film on KBr pellets with t (cm^{-1})) revealed the following characteristic bands: 2837.1–2916.2 (C–H), 1622.0 (C=N), 1604.7 (C=C aromatic), 1247.9–1290.3 (C–O), 991.3–906.5 (C–H vinylic); ^{1}H NMR (300 MHz, DMSO-d_6) d (ppm): 5.35–6.00 (2d, C$\underline{H}_2$=CH–), 8.62 (s, C$\underline{H}$=N–), 6.78–6.85 (2d, CH_2= C$\underline{H}$–), 3.8 (s, OCH_3), 6.96–7.90 (8H of 2 phenyl); Microanalysis of the Schiff's base monomer (Im) $C_{16}H_{15}ON$ (237.16 g. mol^{-1}) gave the experimental % of C (80.96%), H (6.32%) and N (5.90%); UV (Ethanol) k_1 max (e max) = 355 nm (11531), k_2 max (e max) = 262 nm (34691) and k_3 max (e max) = 232 nm (34821).

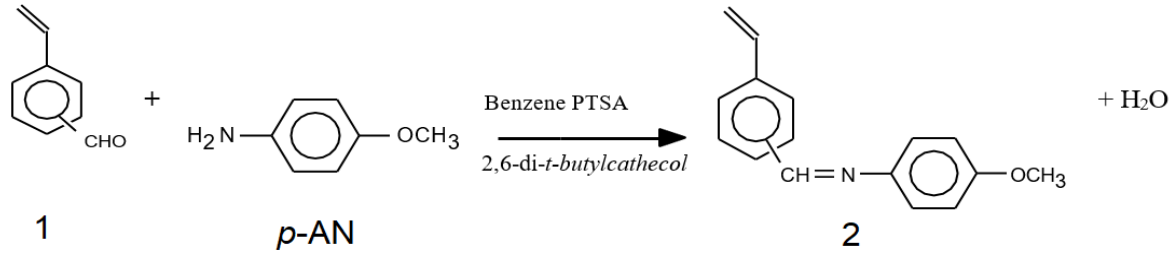

Scheme 2 – Reaction of Schiff's base synthesis.

***Synthesis of copolymers poly (N-(m,p)-vinylbenzylidene-p-anisidine-co-N,N-dimethyl-acrylamide) Cp1* (3) *and Cp2* (4)**

The copolymers Cp_1 (3) and Cp_2 (4) were synthesized by the copolymerization reaction of the obtained imine monomer N-(*m,p*)-vinylbenzylidene-*p*-anisidine (Im) *(2)* with *N,N* dimethylacrylamide (DMA) at two DMA/ Im ratios: 80/20 for Cp_1 and 70/30 for Cp_2 (Scheme 3); giving yield conversion rates of 86% for Cp_1 and 70% for Cp_2, respectively. The copolymerization of DMA and the styrenic imine (Im) was carried out for the following initial molar compositions:

(Cp_1) = DMA: 80% + Im: 20%

(Cp_2) = DMA: 70% + Im: 30%.

In each case, the two comonomers were dissolved in 5 mL of anhydrous dioxane, with 1 wt% of AIBN as the initiator, deliberately chosen to obtain low molecular weights. The polymerization tube containing the reaction mixture was degassed under nitrogen and placed in a thermostated oil bath at 65 °C for two days. The resulting copolymers, appearing yellowish, were precipitated in ether and purified by reprecipitation from concentrated dioxane solutions of Cp_1 and Cp_2 into ether. The final precipitate was dried under vacuum at room temperature.

The obtained copolymers (Cp_1) and (Cp_2) were characterized by FTIR spectroscopy, GPC, DSC and microanalysis.[21] Melting points mp = 218 °C for Cp_1 and mp = 146 °C for Cp_2 were detected (Tottoli Büchi 510) (Table I); IR spectroscopy (film on KBr pellets with t (cm^{-1})) revealed the following characteristic bands: Cp_1: 2852.5–2925.8 (C–H), 1649.0 (C=O), 1624.0 (C=N) and 1245.9 (Caro–O); Cp_2: 2850.6–2922.0 (C–H), 1649.0 (C=O), 1624.0 (C=N) and 1244,0 (Caro–O). Practically, the FTIR

characteristic bands of Cp_1 and Cp_2 appeared in same regions. GPC/THF: (Cp_1)/ g·mol^{-1}: Mn: 20600; Mp: 26500; Mv: 22700 and Mz: 34200; I=1.3. Tg (DSC): 218°C (Cp_2)/ g·mol^{-1}: Mn: 10500; Mp: 13100 Mv: 12200 and Mz: 16400; I = 1.2. Tg (DSC): 146°C. The molecular weights of copolymers Cp_1 and Cp_2 are of the same order of magnitude as those reported for related copolymers synthesized under similar conditions.[1,21,22] The polydispersity indices obtained I < 1.30 indicate that the copolymers exhibit a narrow molecular weight distribution, suggesting homogeneity in chain lengths. The intrinsic viscosimetric molecular weights (Mv) were found Intermediate between the number-average (Mn) and the peak molecular weights (Mp) for both copolymers. The values of incorporation ratios (α^0, β^0) are determined from the microanalysis results. The copolymers' characteristics showed that the molecular weight of Cp_1 is higher than of Cp_2, so using a high percentage of DMA content induced a high copolymer weight (Table 1).[21] Then, the incorporation ratio (β^0) of imine in Cp_2 is increased indicating a high Schiff base content.

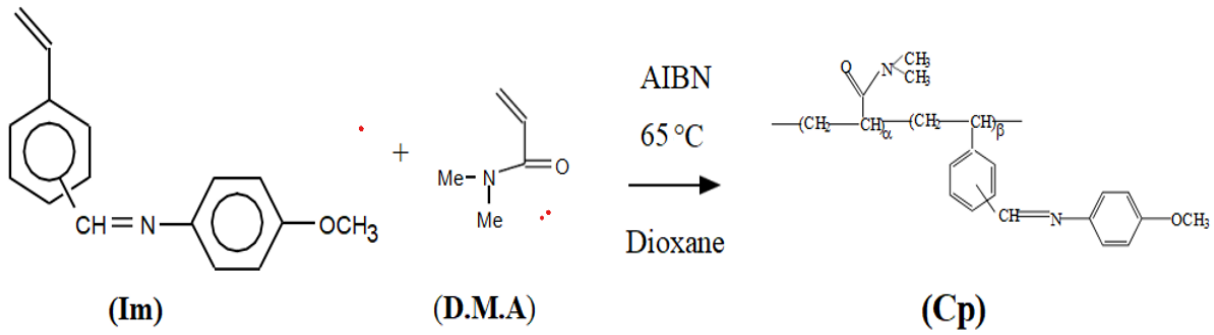

(Im) (D.M.A) (Cp)

Scheme 3 – Synthesis of copolymer carrier poly (*m,p*-vinylbenzylidene-*p*-anisidine- co-*N,N*-dimethyl-acrylamide) *via* copolymerization reaction of Imine (Im) with DMA.

Table 1

Characterization results of copolymers

Comp.	DMA / Im Ratio / %	Molecular weight / g mol^{-1}	Yield / %	Tg / °C	Incorporation ratios
Cp_1	80/20	*Mn* = 20600 *Mp* = 26500 I = 1.3	80.20	218	$\alpha^0 = 0.65$, $\beta^0 = 0.35$ (α0DMA/β0Im=1.86)
Cp_2	70/30	*Mn* = 10500 *Mp* = 13100 I = 1.2	72.52	146	$\alpha^0 = 0.52$, $\beta^0 = 0.48$ (α0DMA/β0Im=1.08)

In vitro release studies of p-AN in heterogeneous media and dissolution tests

The hydrolysis kinetics of Schiff's base monomer (Im) and copolymers (Cp_1) and (Cp_2) were performed in heterogeneous reconstituted gastric (pH 1.2) and intestinal (pH 8) media using a UV-Vis spectrophotometer (2401 PC-Shimadzu apparatus), which was previously calibrated at the maximum absorption wavelength (λ_{max}) of the active agent (*p*-AN). The drug Release experiments were conducted in closed flask, kept at 37 ± 0.5°C and at controlled stirring rate of 500 rpm. At t = 0, 100 mg of monomer or copolymer, were soaked in 100 mL of buffered solution. Samples (1 mL) of drug solutions were analyzed at different intervals using UV-Vis at λ_{max} =272 nm (ε = 1200 L / cm mol) (Fig. 1) for simulated gastric media and at λ_{max} = 295 nm (ε = 2100 L / cm mol) for intestinal media.

The simulated buffer solutions used were prepared according to the standard procedures described in the United States Pharmacopeia (U.S.P. XX) as follows: For the gastric medium (pH 1.2): 80 mL of HCl (1 N), 2 g of NaCl, and distilled water q.s. to 1000 Ml. For the intestinal medium (pH 8): 200.5 mL of HCl (0.1 N), 500 mL of borax solution (0.025 M), and distilled water q.s. to 1000 mL.

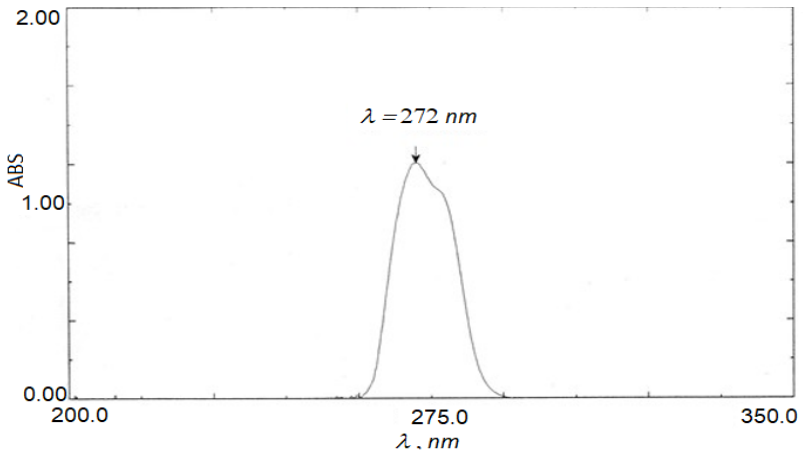

Fig. 1 – UV-Vis absorption spectrum of *p*-anisidine at pH = 1.2 (37°C).

RESULTS AND DISCUSSION

Mechanism of Schiff Base Hydrolysis and pH-Dependent

a. Hydrolysis of Schiff bases in strongly acidic medium at pH ≈ 1.2

We can distinguish the three mechanisms of Schiff base hydrolysis at pH values: 1.2, 4 and 8 (Table 2), with the reaction of the amine product protonation (NH_3^+ in acid, NH_2 in base).

Step 1: Protonation of the imine (K_a) at pH 1.2: Imine protonation occurs rapidly due to the high concentration of H^+ ions; however, the water nucleophilicity is significantly reduced at such low pH due to competition with hydronium ions (H_3O^+). This impairs the rate-determining step, the nucleophilic attack of water on the protonated imine, and slows the hydrolysis rate.

The pH 1.2 used corresponds to a strongly acidic media, in which *the rate determining step 2 in the overall reaction kinetics* of the hydrolysis is the nucleophilic attack of water on the protonated imine forming a protonated carbinolamine (or an oxonium ion OH_2^+), followed by the release of a proton,[12,30,31] according to the following mechanism:

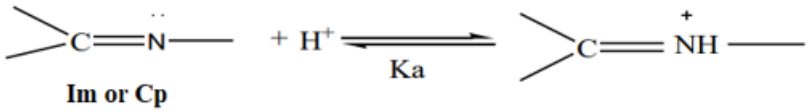

Step 2: Slow Nucleophilic attack (k_1): **A** rapid deprotonation yields carbinolamine. The proton is thus regenerated, which is characteristic of acid-catalyzed mechanisms:

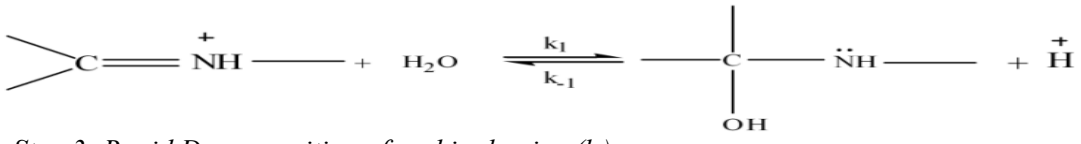

Step 3: Rapid Decomposition of carbinolamine (k_2):

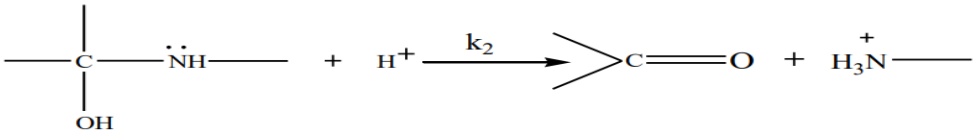

b. Hydrolysis of Schiff bases in strongly acidic medium at pH 4–5

This pH range is moderately acidic medium and provides an optimal balance: Protonation of the imine is favored, while water remains sufficiently nucleophilic. As a result, the hydrolysis proceeds efficiently, with the highest observed reaction rate.

Step 1. Protonation of the Imine favored (Acid-Base Equilibrium – K_a): This protonation is fast and reversible, and is governed by an acid–base equilibrium constant (K_a).

Step 2. Nucleophilic attack by water on the protonated imine (rate-determining) (k_1) This reaction leads to the formation of a carbinolamine intermediate **(**R–CH(OH)–NH–R′**),** this step is acid-catalyzed, and the proton released (H^+) can be recycled in the catalytic cycle.

Step 3. Rapid Carbinolamine decomposition (k_2) with ($k_2 \gg k_1$): Hydrolysis reaction: The amine product (R'–NH_3^+) is protonated with a maximal hydrolysis rate.

c. Hydrolysis of Schiff bases in Basic Medium a*t pH = 8*

However, the pH = 8 range corresponds to a mildly basic medium, in which the hydrolysis proceeds through a different mechanism than in acidic conditions. The imine remains largely unprotonated, and the rate-determining step 2 involves a slow nucleophilic attack by neutral water molecules on the electrophilic carbon of the imine.[21,23] The released amine R'–NH_2 led to very slow hydrolysis rate.

Step 1. No protonation (imine remains neutral): R–CH=N–R'

Step 2. Very slow nucleophilic attack by H_2O or OH^-: R–CH=N–R' + H_2O→R–CH(OH)–NH–R'

Step 3. Fast decomposition of carbinolamine: R–CH(OH)–NH–R' → R–CHO + R'–NH_2

The pK_a of the ammonium/amine equilibrium (R'–NH_3^+ ⇌ R'–NH_2 + H^+) is typically around 9–10. Therefore, at pH = 8, this is slightly below the pK_a, it is close enough that a significant fraction of the amine exists in its unprotonated form; especially in buffered systems. Moreover, protons (H^+) are scarce and as a result, the amine either remains unprotonated by available bases (OH^-) (Table 2).

Theoretical and experimental analyses of the kinetics release of *p*-AN from polymeric carriers

Theoretical analyses of release kinetics

The drug release by diffusion through the matrix depends on three key factors:

1. The rate of liquid penetration into the formulation through the structure of the copolymer matrix (*i.e*., the liquid absorption capacity of DMA);
2. The rate of drug dissolution in the entrapped liquid;
3. The diffusion of the active agent through the DMA matrix.
4. When the active agent is grafted in molecular support, a fourth factor must be considered: the chemical reaction that hydrolyzes the imine link between the drug and its support.

Table 2

Comparative kinetic summary for Schiff's base hydrolysis

Step	Rate Constant	**pH 1.2**	**pH 4–5**	**pH 8**
Imine protonation	K_a	Very fast (fully protonated)	Favored (partial protonation)	Not significant (neutral imine)
Nucleophilic attack by water	k_1	Slow (low nucleophilecity)	Slow but feasible	Very slow (poor electrophile)
Carbinolamine decomposition	k_2	Very fast	Very fast	Very fast
Amine product form	–	R'–NH_3^+ (protonated)	R'–NH_3^+	R'–NH_2 (neutral)
Hydrolysis rate	–	Moderate or reduced	Optimal	Very low

In our case, the synthesized support is a Schiff's base, and its hydrolysis mechanism is as follows:

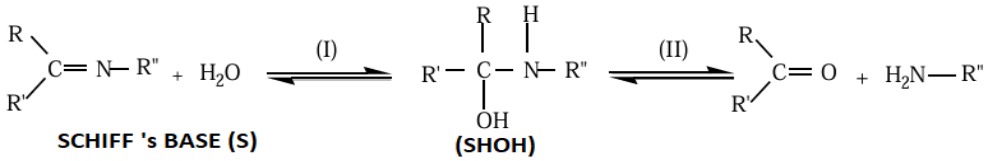

Scheme 4 – Hydrolysis reaction of Schiff's base.

Step 1. Formation of the α-amino alcohol by water addition to the activated double bond, following protonation of the imine nitrogen.

Step 2. Bond rupture of the carbinolamine intermediate, leading to the hydrolysis products.

Determination of the predominant species of (pA) at each studied pH

Quantifying protonated and unprotonated form: Identifying the species to be quantified in each medium is essential, as the release of *p*-AN is studied in three pH media. This determination was carried out using the Henderson-Hasselbalch equation (1)[32]

$$pH = pka + \log\frac{[B]}{[BH^+]} \quad (1)$$

Knowing that pk_a = 5.31, the ratio of unprotonated NH_2 to protonated (NH_3^+) is calculated as:

– At pH = 1.2: $1.2 = 5.31 + \log\frac{[B]}{[BH^+]} \Rightarrow \frac{[B]}{[BH^+]} = 10^{-4,11} \approx 7.9\times10^{-5}$ (2)

$$[BH^+] = 12882\ [B]$$

> 99.99% protonated amine, the neutral species is negligible compared to the protonated form.

– At pH = 8.0: $8.0 = 5.31 + \log\frac{[B]}{[BH^+]} \Rightarrow [B] = 490\ [BH^+]$ (3)

~99.8% unprotonated amine, the protonated form is negligible compared to the neutral form.

Table 3

Quantifying of the Predominant Species of (*p*-AN) at varied Studied pH

pH	Protonation state	Protonated ($–NH_3^+$), %	Unprotonated ($–NH_2$), %
1.2	Fully protonated	~99.99%	~0.01%
4.0	Mostly protonated	~95%	~5%
8.0	Mostly unprotonated	~0.2%	~99.8%

Analysis of the protonation State of p-anisidine as a function of pH values

Understanding the predominant ionic species of *p*-AN at different pH values is crucial for interpreting its release behavior. The Henderson equation allowed us to determine the ratio of the unprotonated to protonated forms at each pH value.[32] From Fig. 2, *p*-AN exists predominantly in its protonated form ($–NH_3^+$) at acidic pH, while at alkaline pH, the unprotonated form is dominant. This protonation shift significantly influences solubility and membrane permeability, thereby affecting its release.

Hydrolysis kinetic study of Schiff's base monomer carrier and its copolymers

To properly investigate the cumulative release of *p*-AN, several important factors must be considered:

1. Hydrophilic Pattern of DMA: a monomer used in matrix to increase water absorption and swelling, which can accelerate the hydrolysis process and consequently promote *p*-AN release.

2. The pK of *p*-AN ($pK_a \approx 5.3$) and Its Solubility: *p*-AN is a primary amine with a pK_a of the conjugate acid of the primary amino group – NH_2 which can be protonated to $–NH_3^+$.

3. The release media pH in drug release studies (acidic or basic) influences the protonation state of *p*-AN. To analyze the protonation state and pKa of *p*-AN at different pH values, here is the key rule:

– If pH < pKa, the protonated form dominates;

– If pH > pKa, the unprotonated form dominates.

Diffusion of the active agent *p*-AN from (Im), (Cp_1) and (Cp_2) at pH = 1.2.

In this work, *p*-AN is grafted on monomer and copolymers to get new controlled formulations, which supports prolonged release. *In vitro* kinetic results of *p*-AN delivery from the monomer (Im)

and its carriers (Cp_1) and (Cp_2) in reconstituted gastric and intestinal media are illustrated in the figures (Figs. 3 and 4). As explained above, the pK of *p*-AN ($pK_a \approx 5.3$) at pH 1.2, when pH ≪ pKa, the protonated form dominates beside its solubility (Table 4). It can be observed that at pH 1.2 < pK_a, *p*-AN is mostly protonated, hence more water-soluble and potentially more diffusible; while in basic media at pH > pK_a, *p*-AN is mostly unprotonated, more lipophilic, and may have reduced solubility. The pH 1.2 corresponds to a strongly acidic medium, in which the rate determining step 2 is the nucleophilic attack of water (k_1) on the protonated imine, according to the mechanism cited above. The protonation is very rapid and complete, the amine exists in its protonated form ($R'–NH_3^+$). Thus, water is poorly nucleophilic due to the high acidity caused by the excess of hydronium ions that reduce the free water molecules, and consequently, overall kinetics are slowed despite the activation.

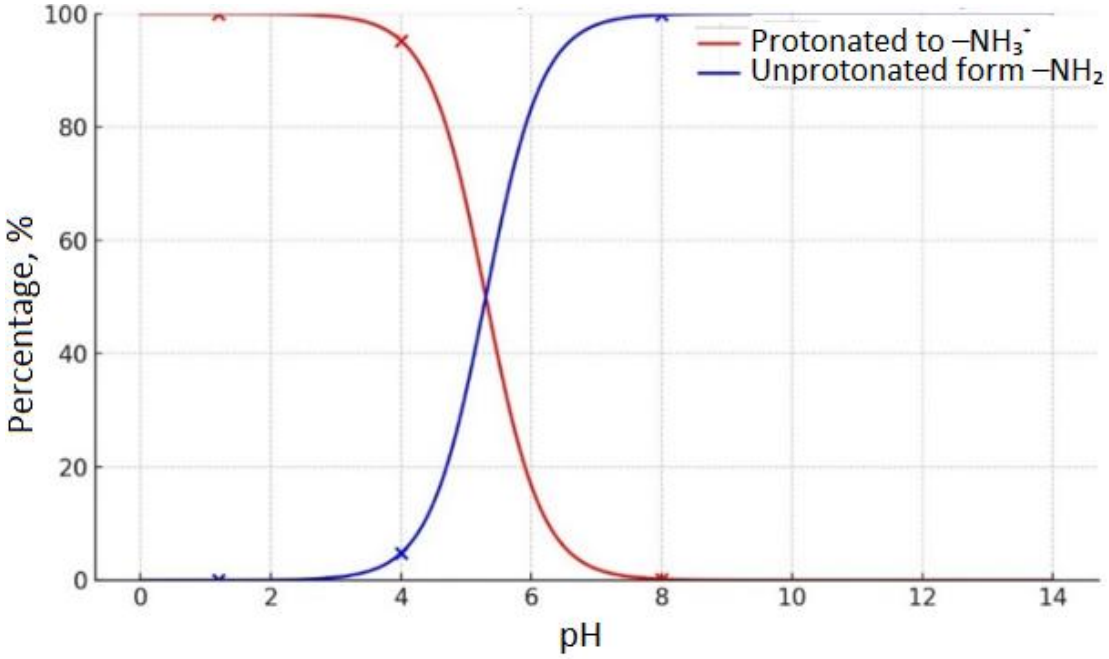

Fig. 2 – Distribution of the of p-anisidine as a function of pH.

Table 4

The Predominant form of *p*-AN with comparison to pKa at studied pH

pH	Comparison to pKa (5.3)	Dominant Form of *p*-AN
1.2	pH ≪ pKa	Protonated ($–NH_3^+$)
4.0	pH < pKa	Mostly Protonated
8.0	pH > pKa	Unprotonated ($–NH_2$)

According the kinetic results, it is obvious that only the active agent *p*-ANH^+ is released as function of time during the hydrolysis of Schiff's base or copolymer supports. From the release profiles shown in Fig. 3, the percentages of *p*-AN released from the studied carriers in acidic media at pH 1.2 are, at almost every time point, ranked in the inverse order of their molar masses:

$$\%(p\text{-AN})_{released}\ (Cp_1) < \%(p\text{-AN})_{released}\ (Cp_2) < \%(p\text{-AN})_{released}\ (Im) \quad (4)$$

$$(Mn\ (Cp_1) = 20600) > (Mn\ (Cp_2) = 10500) > (M\ (Im) = 1) \quad (5)$$

The released amounts (*p*-AN)eq at equilibrium are reached between 150 and 175 minutes for all three studied compounds. These amounts decrease with increasing molar mass, they are inversely correlated

with the molar mass: (Cp_1): 28% (*p*-AN)eq; (Cp_2): 54% (*p*-AN)eq and (Im): 70% (*p*-AN)eq, after approximately three hours of release kinetic study (Fig. 3). These results can be explained by the hindered diffusion of *p*-AN from the exterior of the carrier through the macromolecular entanglement characteristic of the copolymers. Consequently, the amounts of *p*-AN released are not only lower but also appear over longer time intervals. The absence of a coiled macromolecular chain structure in the Schiff's base monomer (Im) particles facilitates the diffusion of *p*-AN via hydrolysis of imine-link, resulting in higher release rate.

The release of cation *p*-ANH^+ produced from hydrolysis of azomethine function of imine monomer in acidic media pH = 1.2, presents higher release percentage (%) than the basic media pH = 8. This is attributed to the rapid hydrolysis of the imine linkage (C=N) in the Schiff's base under acidic pH conditions,[12-20] resulting in 65% of cumulative release after two hours for Im, 52% for Cp_2 and 25% for Cp_1. At pH 1.2, the majority of *p*-ANH^+ is released as a result of the hydrolysis of the imine function (Im) or the pendant Schiff base groups of copolymers Cp_1 and Cp_2. As reported by Hu *et al.*, imine (C=N) linkages are particularly prone to acid-catalyzed hydrolysis, releasing drugs in a controlled manner, which supports our observation of the enhanced degradation of Schiff base carriers in acidic conditions.[22]

This pH-sensitive hydrolysis mechanism has already been investigated in our previous studies.[1,12–21,23,24,30,31] It can be observed that in acidic media, more monomer Im content generally leads to faster or higher cumulative release, due to increased water diffusion and hydrolysis of group pendant of Schiff base in copolymer (Im content: Cp_1 70% and Cp_2 80%, Table 1). Whatever the pH, the hydrolysis kinetic constant of mono-imine (Im) is higher than those of copolymers in both media, indicating that Im is rapidly hydrolyzed compared to copolymers (Cp_1) and (Cp_2). These kinetic results indicated that the *p*-AN release from the monomer carrier (Im) were faster than those from copolymers. After one hour, the percentage of drug released in simulated media at pH 1.2 from (Im) reached 50% and only 42% and 18% for Cp_2 and Cp_1, respectively.

The kinetic results showed that the copolymer hydrolysis proceeded more slowly and exhibited a delayed release of *p*-AN compared to the imine monomer (Im). This observation is consistent with theoretical expectations, as the release from copolymer carriers involves an additional step – diffusion through the macromolecular matrix. Such release behavior aligns well with the established principles of mass transfer in polymeric systems. The slower release observed with Cp_1 and Cp_2 is primarily attributed to the additional diffusion step required for the penetrating liquid medium to traverse the entangled macromolecular networks of the copolymers, which significantly hinders the diffusion of the active agent.

The difference in diffusion rate and release kinetics between Cp_1 and Cp_2 can be attributed to their disparity in molecular weights. Cp_1 exhibits a higher molecular mass than Cp_2, due to its higher DMA content (%DMA/Im ratio of 80/20 for Cp_1 *vs* 70/30 for Cp_2). This higher DMA content leads to a more coiled and densely packed polymer structure, which hinders the diffusion of the penetrating liquid and slows down drug release. These kinetic findings are consistent with molecular weight distributions previously determined by GPC.

A similar trend was observed in our previous study,[21] where significantly lower release values were recorded for the copolymeric systems: at pH = 4 medium, hydrolysis of the imine linkage led to 65% drug release from Im, compared to only 30% and 20% for Cp_2 and Cp_1, respectively. This further supports the notion that the imine linkage in the monomeric form is more susceptible to acidic hydrolysis compared to its grafted counterparts. However, in both acidic and basic media, despite the expectation that a higher DMA content would enhance water absorption and promote faster hydrolysis of the imine linkage – owing to the hydrophilic nature of DMA – the experimental data show that the drug release rates were actually lower for Cp_1 compared to Cp_2 and the Im monomer.

This observation suggests that while DMA facilitates hydrolysis through increased swelling and water uptake, the overall release rate is governed by a balance between enhanced hydrolysis and restricted diffusion due to the denser polymer network associated with higher molecular weight. Therefore, the dominant factor in Cp_1 appears to be its compact structure, which overrides the hydrolysis-promoting effect of DMA. Concerning the drug release from copolymers, it was observed a notable burst effect particularly for Cp_2. This effect was due inevitably to its low mass and high percentage of monomer support of Im (%DMA/Im: 80/20 for Cp_1), which can be on the macromolecule chain extremities.

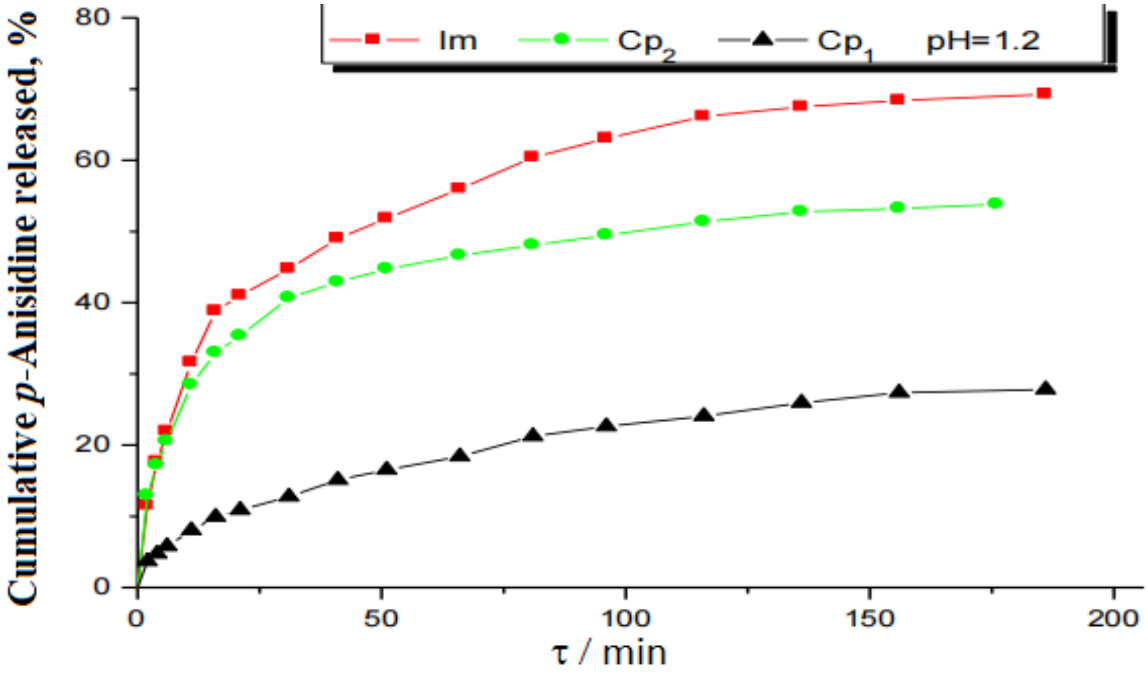

Fig. 3 – % Cumulative release of *p*-AN from Im, Cp_1 and Cp_2 as function of time at pH= 1.2.

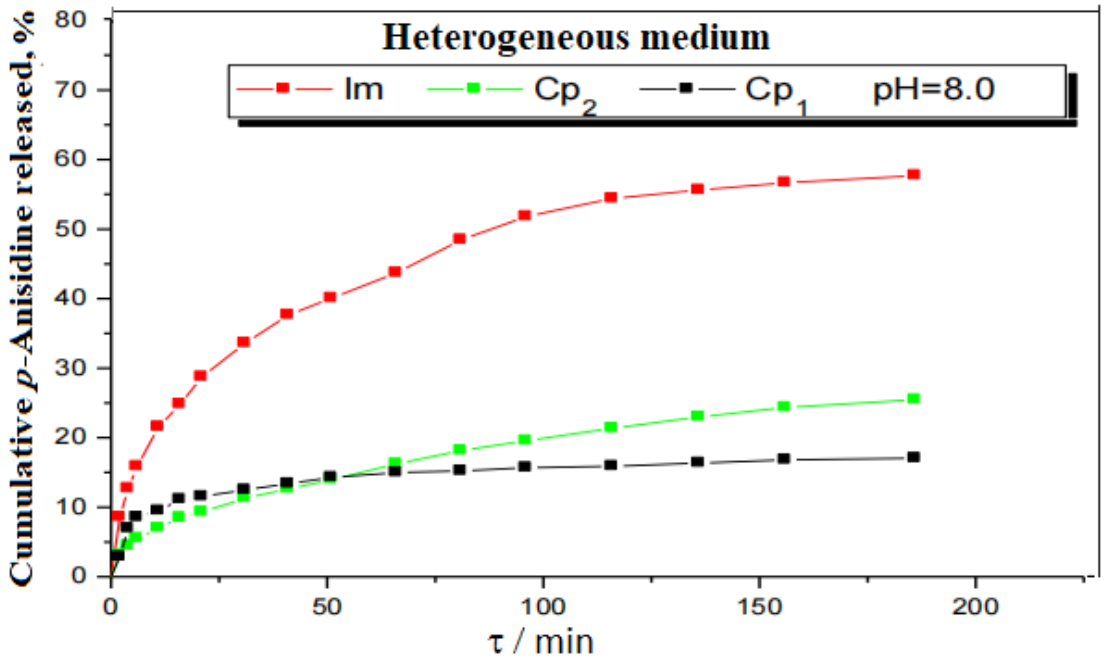

Fig. 4 – % Cumulative release of *p*-AN from Im, Cp_1 and Cp_2 as function of time at pH = 8.

However, in simulated basic medium at pH 8, the percentage of drug release from Im after two hours reached 55%, compared to only 23% and 13% for Cp_2 and Cp_1, respectively (Fig. 4). Furthermore, *p*-AN release from the Schiff base monomer in basic conditions was slower than that observed in acidic conditions, due to the slower hydrolysis of the imine (C=N) linkage in basic media. This observation is consistent with the behavior previously discussed in the acidic medium. As shown by Liu *et al.*, imine bonds exhibit significantly different hydrolysis kinetics depending on pH: rapid hydrolysis in acidic media, intermediate rates at neutral pH, and slower kinetics in basic conditions.[20]

In fact, the release kinetics cannot be described by simple classical models. Regardless of the medium considered and pH conditions, the

release profiles do not follow conventional kinetic orders. This was confirmed by attempting to fit the experimental data to reaction orders n = 0, 1, and 2. As an example, the plots of these kinetic models show a clear deviation from linearity at pH 1.2 (Fig. 5), indicating a poor fit. Additional fitting for other pH are provided in the supplementary Materials.

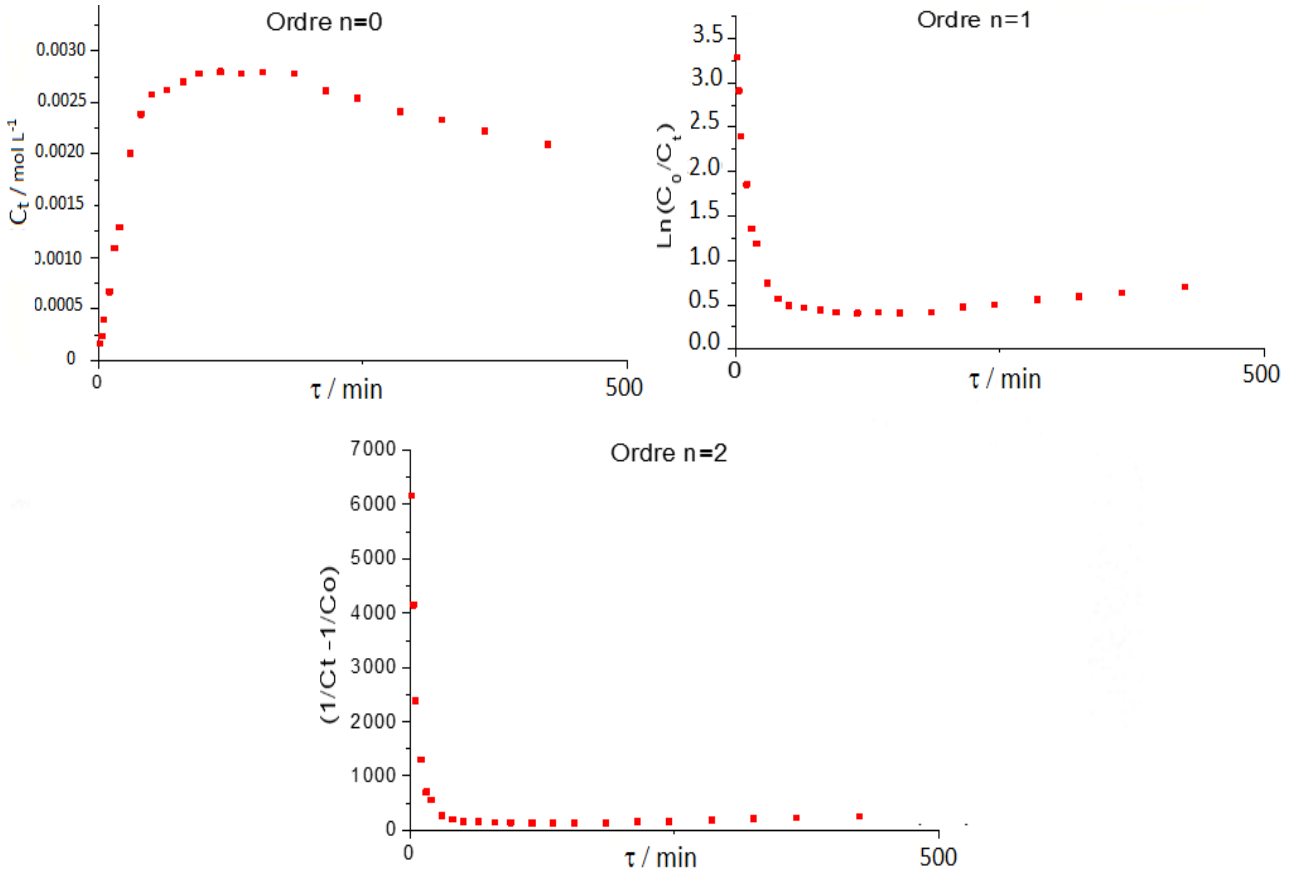

Fig. 5 – Cumulative concentration C_t, Ln (C_0/C_t) and (($1/C_t - 1/C_0$) of *p*-Anisidine released from monomer carrier monoimine (Im) as function of time in pH = 1.2, respectively.

The diffusion behavior of the release was demonstrated by plotting the percentage of drug released (%) as a function of the square root of time, which resulted in a linearization of the experimental data at short times (Fig. 6). The rate-limiting step in this kinetics was found to be diffusion-controlled, indicating that the drug release mechanism is governed by diffusion according to Fick's laws.

Following the kinetic analysis, we now focus on the determination of the mass of the diffusing substance at infinite time (equilibrium), denoted as M_∞. The mass of diffusing at time t M_t compared to the mass of diffusing substance at equilibrium M_∞ are determined by a relation derived from analytical solution of Fick's second law for diffusion, as given in Crank's model "The Mathematics of Diffusion",[32] the expression of the remaining fraction of substance yet to diffuse at time t, *i.e.*:

$$\frac{M\infty - Mt}{Mi} - \frac{6}{\pi^2}\sum_{n=1}^{\infty}\frac{1}{n^2}\exp\left(-\frac{Dn^2\pi^2 t}{R^2}\right) \qquad (6)$$

where: M_t is presumably the initial amount of substance diffused at time t; M_∞ is the amount diffused at infinite time (equilibrium) and R is the macromolecule grains radius.

The plot of the function log (M_t/M_i) = f (1/t) allows us to extrapolate the equilibrium value at infinite time, during the period when the diffusion coefficient D becomes constant. By extrapolating to infinite time, we can estimate M_∞ *i.e.*, the total amount of active substance eventually released. This calculation was performed for all the studied compounds. Figure 7 presents an example of the m_∞ determination for the Im at pH = 1.2.

We have: log (M_t/M_i) = exp [Ln (M_t/M_i)] = m_∞/m_i = exp (–X) =Y $\Rightarrow$ m_∞ = Y. m_i

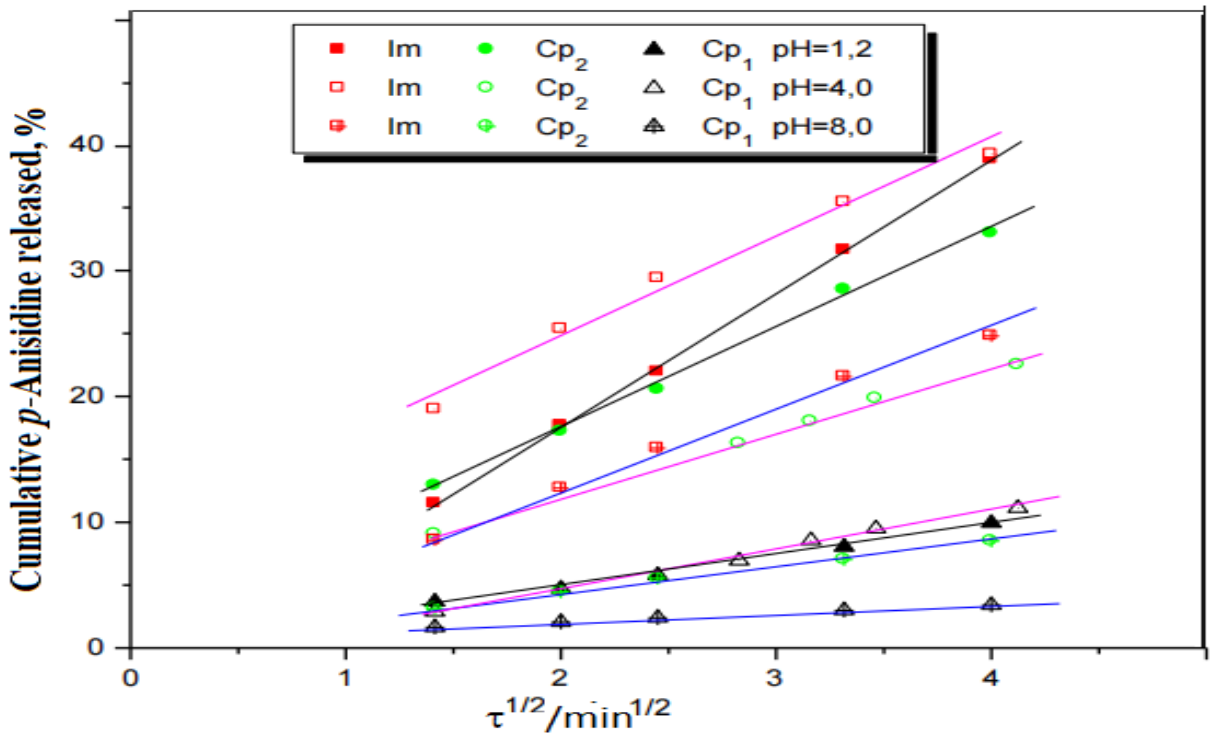

Fig. 6 – % *p*-AN release from monomer and copolymers carriers as function of square root of time.

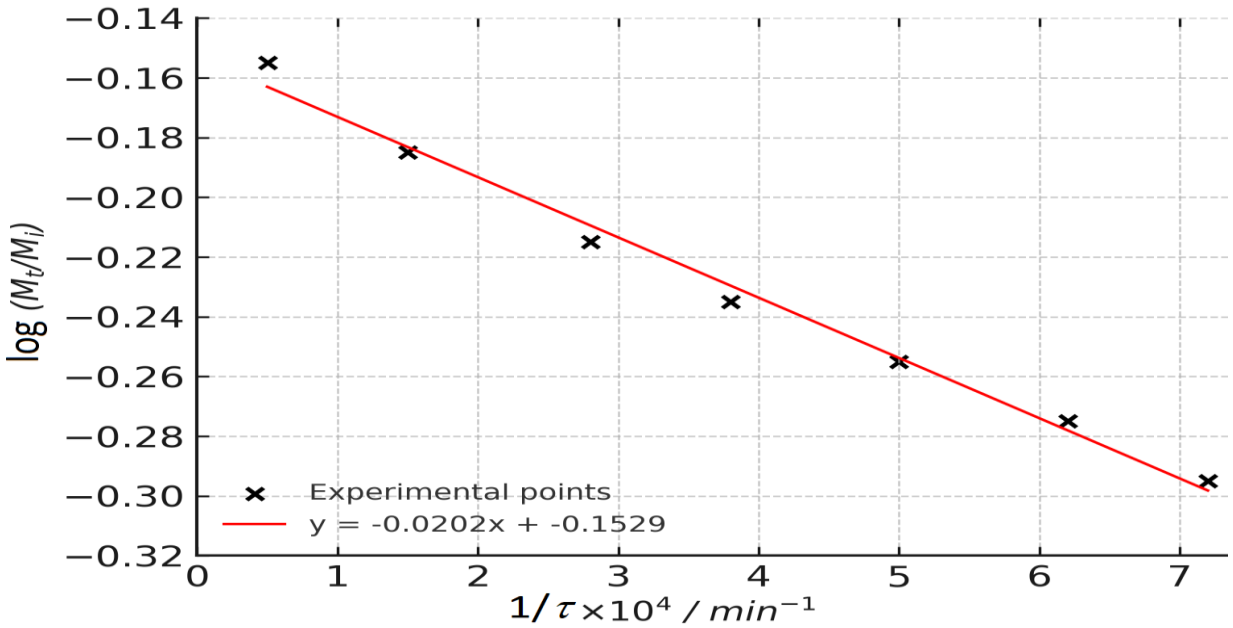

Fig. 7 – Cumulative log (M_t/M_i) of *p*-AN released from Im as function of time in pH 1.2.

Table 5 reported the values of infinity's weights of $(\%\ p\text{-AN})_\infty$ released at an infinite time, in both of gastric and intestinal media. It is observed that molar mass has a significant effect on the drug release rate: higher molar mass resulted in the lower amount of drug released from polymeric carriers.

This effect is due to the more entangled and densely structure of the copolymer Cp_2, which exhibits lower number-average molecular weights (Mn) and (Mp), tends to release a greater amount of drug compared to Cp_1. As shown in Table 5, the equilibrium release masses (m_∞) are inversely proportional to the average molar masses of the two copolymers, regardless of the pH values.

Table 5

Values of infinities drug weights from carriers in gastric and intestinal media

pH	Carrier	m_∞ (*p*-AN) / mg	Initial *p*-AN weight / mg	Initial carrier weight / mg	$(p\text{-AN})_\infty$ / %	Mol. weight / g mol^{-1}
1.2	Im	35.88	51.12	100	69	–
	Cp_1	18.82	28.75	100	51	*Mn* = 20600 *Mp* = 26500 I = 1.3
	Cp_2	28.50	35.14	100	27	*Mn* = 10500 *Mp* = 13100 I = 1.2
4.0[a]	Im	42.79	51.12	100	65	–
	Cp_1	13.89	28.75	100	35	*Mn* = 20600
	Cp_2	23.47	35.14	100	25	*Mn* = 10500
8.0	Im	48.21	51.12	100	58	–
	Cp_1	09.31	28.75	100	25	*Mn* = 20600
	Cp_2	19.10	35.14	100	16	*Mn* = 10500

[(a)] correspond to data previously reported at pH 4 in our earlier study and are presented here for comparison purposes. [21]

Kinetic modeling of drug release using Higuchi and Korsmeyer-Peppas equations

To analyze the drug release kinetics, the cumulative release data versus time were fitted to Higuchi and Korsmeyer-Peppas equations.[33,34–38] Higuchi described drug release by an equation of the type:

$$Q_t = k_H . t^{1/2} \quad (7)$$

where, Q_t is the cumulative percent of drug released at time t and k_H is the dissolution constant characteristic of the equation. The cumulative % *p*-ANH^+ release was proportional to square root time suggesting that the drug release from carriers (Im, Cp_1 and Cp_2) was diffusion controlled (Fig. 6). The Drug release constants and correlation coefficients of kinetic Modeling using Higuchi and Korsmeyer-Peppas equations were reported in Table 6.

The obtained results that the Higuchi release constant (k_H) ranges from 9.81 min$^{1/2}$ to 0.837 min$^{1/2}$. The release constants of Imine in the different pH media were higher compared to those of Cp_2 and Cp_1, which is fully consistent with theoretical expectations. We observed that the constant *c* is positive for all the release kinetics. Regarding the Korsmeyer-Peppas results, the kinetic constants ($k_{K\text{-}P}$) can not be directly compared since they depend on the exponent n, which varies among the different release kinetics studied. Furthermore, the value of n allows us to specify the diffusion mechanism and determine whether it follows Fickian behavior.

Table 6

Kinetic constants and Correlation coefficients of *p*-AN release from (Im), (Cp_1), and (Cp_2)

Formulation	pH	Higuchi's Equation		Korsmeyer–Peppas's Equation		
		$Q = k_H t^{1/2} + c$	r^2	*n*	*k* (min^{-n})	r^2
(Im)	1.2	y = 9.810x – 1.280	0.9950	0.555	0.0200	0.9938
	4.0	y = 9.761 x + 3.290	0.9646	0.327	0.0060	0.9957
	8.0	y = 6.340x – 7.810 x 10^{-4}	0.9978	0.508	0.0050	0.9968
(Cp_1)	1,2	y = 2.443x – 0.013	0.9976	0.482	0.0012	0.9938
	4.0	y = 2.777x – 0.446	0.9896	0.583	0.0040	0.9900
	8.0	y = 0.837x +0.241	0.9770	0.297	0.0016	0.9686
(Cp_2)	1.2	y = 8.265x + 0.527	0.9978	0.445	0.0080	0.9955
	4.0	y = 5.475x + 0.588	0.9959	0.386	0.0048	0.9891
	8.0	y = 2.110 x + 0.130	0.9979	0.462	0.0011	0.9973

The obtained values showed that the exponent n varies from 0.44 to 0.55, which is close to 0.5 for the compounds Im, Cp_2 (at pH 1.2 and 8.0), and Cp_1 (at pH 1.2). For Im and Cp_2 (at pH 4.0), the results indicate that n ranges from 0.33 to 0.38, while for Cp_1 (at pH 4.0 and 8.0), n varied between

0.3 and 0.58. Finally, modeling based on the Korsmeyer-Peppas equations allowed us to conclude that the release from the synthesized carriers exhibits Fickian diffusion behavior.

Kinetic Profile and Interpretation

The kinetic data showed that only *p*-AN is released over time, indicating that the carrier matrix is not monomer units or degradation products, only the active molecule; and the hydrolysis-driven release is likely the mechanism, especially if imine linkages are involved in conjugating *p*-AN to the matrix.

By comparing Im, Cp_1, and Cp_2: the monomer Im might show a faster but more limited release, lacking the structural stability or swelling properties of copolymers based on their composition (The higher DMA content led to a faster release due to higher swelling).

The higher molecular mass led to slower diffusion of the liquid medium into the polymer matrix, and consequently, to a low drug release rate. This effect is attributed to the higher viscosity and the denser crosslinking of the polymer chains associated with the higher DMA content (Table 7):

Table 7

Key considerations for data analysis

Factor	Effect on *p*-AN Release
DMA content	Increases hydrophilicity, swelling and thereby higher release rate
pH vs pK_a of *p*-AN	Controls solubility and diffusion; at pH 8, *p*-AN is less ionized
Solubility of *p*-AN	Caps cumulative release; needs to be quantified
Polymer structure (Im *vs* Cp_1/Cp_2)	Affects hydrolysis rate and diffusivity of *p*-AN

Comparative study between homogeneous and heterogeneous media

This study investigates the hydrolysis kinetics of the *p*-AN-based monomer (Im) and its copolymers in heterogeneous acidic (pH 1.2) and basic (pH 8) media. The main is to elucidate the hydrolysis mechanism and drug release behavior in order to determine the effect of copolymerization on the hydrolysis rate constant, and to compare the release kinetics of *p*-AN from carriers in two reaction media at different pH values (37 °C). The study was conducted in two types of media:

(1) *Heterogeneous media*, consisting of buffer solutions at pH 1.2, 4.0 and 8.0;

(2) *Homogeneous media*, composed of ethanol/water (80% *v/v*) mixtures, at pH 4–10.0 (*see ref. 1*).

The UV-Vis spectra obtained during the hydrolysis study of the Schiff base in homogeneous media,[1] showed that this class of compounds exhibits four characteristic absorption bands (I to IV), with two Bands I and II corresponding to $n\rightarrow\pi^*$ transitions at wavelengths distinct from those of the parent aldehyde. These bands appear clearly in the imine (Im) spectrum and remain unchanged during the initial time of hydrolysis in the hydro-ethanolic medium. In our previous study, a comparison of the UV spectra of Im, *p*-anisidine, and *m,p*-vinylbenzaldehyde confirmed that Band I, corresponding to the $n\rightarrow\pi^*$ transition of the imine function, is the most suitable for monitoring hydrolysis kinetics due to its sensitivity to changes in the imine function. The decrease in intensity of Band I during hydrolysis reflects the cleavage of the imine function. For Cp_2, the initial UV spectrum showed four characteristic bands typical of aromatic Schiff's bases. The disappearance of Band I confirmed complete hydrolysis, resulting in spectra corresponding to the amine and aldehyde products (Scheme 4). The presence of isosbestic points i1 and i2 throughout the process suggests a direct conversion without accumulation of intermediates, especially the α-amino alcohols, during the hydrolysis process (Scheme 4). The hydrolysis of these Schiff's base followed apparent first-order kinetics, as evidenced by the quasi-constancy of ($t_{1/2}$) whatever of the initial concentration (C_o) of either the free imine (Im) or the copolymer carriers (Cp).[1] It is noted that by varying the pH medium, the kinetic constants (*kobs*) of copolymers at four values of pH is lower than *kobs* of Im since the concentration of imine group in copolymers depends on the degree of incorporation (β^0). For example, in basic pH = 7.91, the mean value of k_{obs} are respectively 9.60×10^{-4} s^{-1} for Im, 5.84×10^{-4} s^{-1} for Cp_1 ($\beta 0$= 35%) and 3.5×10^{-4} s^{-1} for Cp_2 (β^0 = 48%) (Table 8). In fact, at initial time, the imine concentration in copolymer is significantly lower than pure imine.

By comparing Cp_1 and Cp_2, the value of k_{obs} is in agreement with copolymers' imine content, so higher is the incorporation rate (β^0), lower is the kinetic constants (*kobs*). The results showed obviously that at same pH value, the hydrolysis constants of copolymers are lower than of the monomer (Im). It is coherent that the copolymer backbone affects significantly the hydrolysis constant. As a result, copolymers and especially Cp_2 exhibited delayed *p*-AN release since the hydrolysis constant is decreased. The $k_\Psi(Im)/k_\Psi(Cp)$ ratios, being slightly greater than 1, indicate that the molecular weights of the copolymers are relatively low, and that water access to the iminium groups is mildly hindered. Thus, Cp_2, which has approximately half the molar mass of Cp_1, undergoes hydrolysis more easily. There is a good correlation between k_Ψ (Cp_1), k_Ψ (Cp_2), and the corresponding number-average molar masses. Similar results have been reported for the hydrolysis, where the highest ratio was 9 with a mass Mn = 90.000 g mol^{-1}.[31]

During the hydrolysis process, the evolution of the copolymers UV spectra facilitates the clarification of the reaction. Once the total reaction has been achieved, a mole of copolymer (Cp) gives an equal amount of aldehyde (VBA) based copolymer and β^0 mole of *p*-AN (Scheme 5). To support the interpretation of this results, the characteristic pH-rate profile for Schiff bases illustrated in our previous study,[21] showing two distinct zones: an acid-catalyzed region (A) from pH 4.65 to 7.71, and a basic plateau (P) from pH 7.71 to 9.91, where the hydrolysis rate becomes pH-independent.

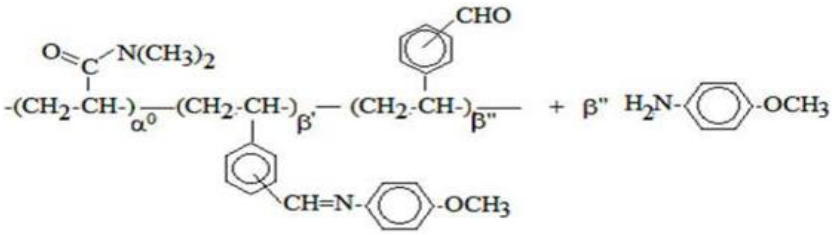

Scheme 5 – Partial hydrolysis of copolymers.

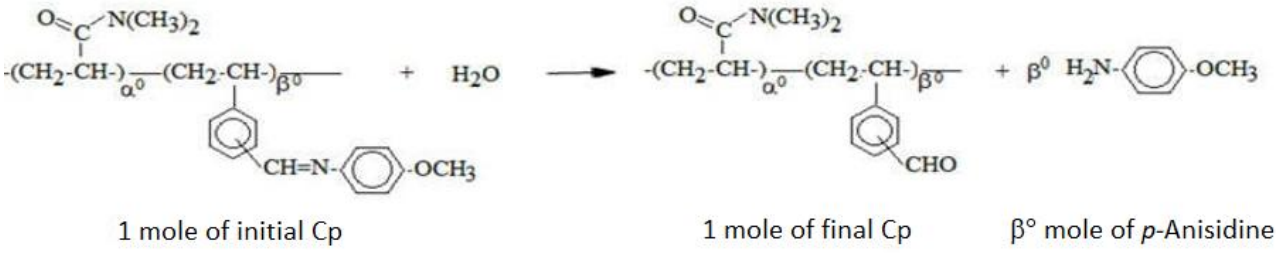

Scheme 6 – Complete hydrolysis reaction of copolymers.

To complete this section, Fig. 8 summarizes the collected release data of Im, Cp_1, and Cp_2 at 37 °C from the comparative study in both homogeneous (pH 7.71) and heterogeneous (pH 8.0) media, highlighting the impact of carrier type and medium on sustained *p*-AN release. The kinetics results of drug release can be described by a classical kinetic equation in homogeneous media, however, the process can be considered controlled by diffusion according to Fick`s laws in heterogeneous media.

Table 8

Hydrolysis kinetic parameters of Im, Cp_1 and Cp_2.1

pH	(Im)		(Cp_1)		(Cp_2)		$\frac{k_\Psi}{k_{Cp1}}$	$\frac{k_\Psi}{k_{Cp2}}$
			Mn = 20600 g mol^{-1}, β^0 = 35%		*Mn* = 10500 g mol^{-1}, β^0 = 48%			
	k	D^0	$k \times 10^4$ / s^{-1}	D^0	$k \times 10^4$ / s^{-1}	D^0		
4.65	790	1.62	455	0.10	294	0.22	1.74	2.68
6.18	53.0	1.66	52.0	0.14	26.2	0.26	1.02	2.02
7.71	9.60	1.68	5.84	0.22	3.50	0.19	1.64	2.74
9.91	11.0	1.50	8.00	0.16	3.97	0.27	1.38	2.77

The comparison of these two studies showed that, for the same time of immersion, the drug release is more important in heterogeneous media, where the quantities of *p*-AN released are not only weaker but appear at longer intervals of time. Similar conclusions were obtained in a previous study.[21] For the latest study discussing about the kinetic hydrolysis of Schiff's base in homogeneous media, the results showed that the hydrolysis follows first-order kinetics and is extremely dependent on both pH and carrier structure. Indeed, the hydrolysis of the copolymers led to a delayed release of *p*-AN. Regardless of the pH, the hydrolysis rate constant of the Im is consistently higher than those of the copolymers, indicating that Im undergoes faster hydrolysis than its polymeric counterparts.

In the homogeneous medium, a rapid appearance of solubility peaks of *p*-AN is observed, which in fact decreases its therapeutic time, as the maximum release is reached within just 80 minutes. In contrast, in the heterogeneous medium (Figs. 3 and 4), the *p*-AN release is significantly more delayed, allowing for a prolonged availability of the active agent over time. For an immersion time of 10 minutes, the percentages of *p*-AN released in the homogeneous medium were approximately 42%, 28%, and 20% for Im, Cp_2, and Cp_1, respectively.[1] The maximum of %*p*-AN release is reached after 80 minutes, with values of 98%, 87%, and 81% for Im, Cp_2, and Cp_1, respectively. In contrast, in the heterogeneous medium, the initial part of the release process exhibited almost vertical tangents, with around 17% of percent release for the monomer, 09% for Cp_1 and 06% for Cp_2. Quantitatively, the mass of *p*-AN released at equilibrium (after 160 min) was higher in the homogeneous medium: Im: 100% (*vs* 57% in heterogeneous), Cp_2: 87% (*vs* 27%) and Cp_1: 94% (*vs* 15%). The calculated improvement ratios (homogeneous *vs* heterogeneous) for total release were: Im: 1.75, Cp_2: 3.23 and Cp_1: 6.27. The sustained-release effect is therefore notably improved in the heterogeneous medium. The availability of *p*-AN in the medium is considerably enhanced, resulting in a more prolonged therapeutic effect.

A clear distinction in behavior of release kinetics and hydrolysis efficiency was observed between the two media. In the homogeneous medium, the hydrolysis follows apparent first-order kinetics, and adheres to the established imine hydrolysis mechanism across various pH values. The carriers were solubilized in the medium, which resulted in rapid drug release, reaching maximum release within the first 80 minutes. This rapid release, while efficient, reduces the therapeutic availability of the active agent. The hydrolysis rate was found to be highly pH-sensitive, and the pH-rate profile was established.

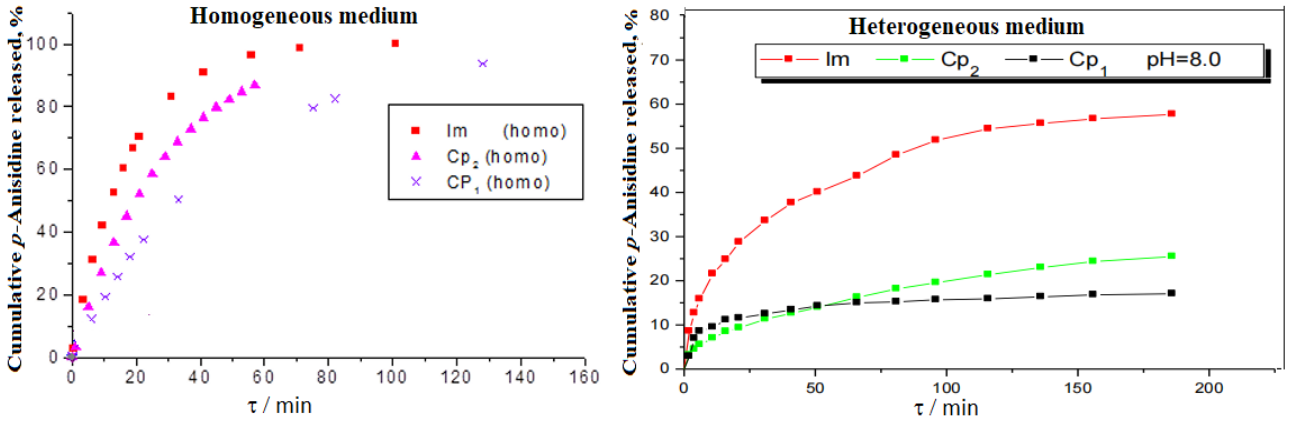

Fig. 8 – % *p*-AN released as a function of time at pH 7.71 in the homogeneous medium and at pH 8.0 in the heterogeneous medium for Im, Cp_1, and Cp_2 at 37 °C.

In contrast, the drug release was significantly delayed in heterogeneous media, where the carriers remain insoluble. This "retard effect" was due to a sequence of diffusion-controlled steps that governed the overall process: Hydration of the polymer surface with formation of a water film; Penetration of the external aqueous phase into the polymer matrix; Chemical hydrolysis of the imine bond, releasing *p*-AN inside the matrix; and Diffusion of the released *p*-AN through the hydrated polymer into the medium. The pH had a secondary effect compared to the dominant role of diffusion and matrix permeability. In fact, the homogeneous study was achieved through the addition of ethanol to the medium. However, since the

human body does not naturally contain such levels of alcohol, a more suitable approach would be to graft the active agent onto biodegradable carriers and nanoparticles, thereby avoiding the toxicity issues associated with insoluble supports. Further, this comparative study demonstrates that release in homogeneous media is kinetically favorable but temporally limited**,** whereas heterogeneous media improved the availability of the active, which contributes to a more sustained therapeutic effect. The overall hydrolysis mechanism remains consistent, dependent on the imine bond reactivity, but the media-specific determine the release rate and duration. Consequently, for applications requiring extended drug release, heterogeneous systems offer a pronounced retard effect**,** despite lower initial release percentages (Table 9).

Table 9

Summary of the comparative study between both media under different conditions

Criteria	Homogeneous medium	Heterogeneous medium
Solvent system	Ethanol/Water (80% *v/v*)	Aqueous with insoluble polymer supports
Solubility of carriers	Fully soluble	Insoluble
Kinetic order	Apparent first-order	Diffusion-controlled, multi-step process
Carrier effect	Significant	Major influence due to insolubility
pH sensitivity	High (clear pH–rate profile)	Moderate
mechanism	Direct imine hydrolysis	Hydration- Penetration -Hydrolysis –Diffusion
Time to max release	Fast (≈80 minutes)	Delayed (≥160 minutes)
Maximum release	Im: 100%,Cp_2: 87%, Cp_1: 94%	Im: 34%, Cp_2: 27%, Cp_1: 10%
Therapeutic availability	Rapid initial burst	Extended and controlled release
Application	Immediate-release applications	Sustained/controlled-release formulations

Hydrolysis in homogeneous media

The hydrolysis of Schiff's base and its copolymers, was studied in a homogeneous ethanol/water medium (80% v/v) at 37°C and pH 4.0–10.0.

The reaction followed first-order kinetics for all compounds tested. The rate of hydrolysis was highly dependent on both the monomer or copolymer carrier and the pH of the medium.

A pH–rate profile was established, showing significant sensitivity of hydrolysis rates to pH changes, indicating that the imine function's stability varies with environmental conditions.

Hydrolysis in heterogeneous media

The hydrolysis of imine Im and its copolymers, was investigated in a heterogeneous medium at 37 °C and pH 1.2, 4.0 and 8.0, where the polymeric supports remain insoluble.

The release process followed a diffusion-controlled mechanism, rather than purely kinetic, due to the solid nature of the supports. In fact, hydrolysis involved four distinct stages cited above.

The insolubility of the carriers significantly slowed the release, enhancing the sustained release effect and delaying the maximum of *p*-AN release.

The pH had a secondary effect compared to the dominant role of diffusion and matrix permeability.

Overall, the heterogeneous medium provided a more pronounced delayed-release behavior, making it suitable for applications requiring controlled or prolonged delivery.

CONCLUSION

In the present paper, *p*-anisidine was modified by grafting it on monomer based on (*m,p*)-vinylbenzaldehyde and copolymerization with dimethylacrylamide. The drug release from these formulations was studied in acidic (pH = 1,2) and basic (pH = 8) media and the results demonstrated that *p*-AN release was strongly affected by the copolymer supports. Then the results showed the importance of the molecular mass of polymers on the drug release constant. Concerning the drug release from copolymers, we deduced that; both in acidic and basic media; released drug percent were lower in the case of Cp_1 than Cp_2's and then those of Im. Certainly, it was due to them high mass which includes the hydrophilic co-monomer "dimethylacrylamide". The hydrolysis of the imine function demonstrates that the monomer carrier undergoes hydrolysis more rapidly than the corresponding copolymers in both media. This was attributed to the polymeric structure, which imposes steric and diffusional barriers that slow the release of

the active agent. The pH of the release medium mainly affects the solubility of *p*-AN. A comparative analysis of both studies involving the same carriers reveals an important finding: the retardation effect is more significant in the heterogeneous medium. The insolubility of the carriers leads to a slower release of the active agent, due to the involvement of at least four sequential steps, where diffusion acts as the rate-limiting process. The pH had a secondary effect compared to the dominant role of diffusion and matrix permeability. These results reflect the strong impact of diffusion limitations in heterogeneous media. However, the controlled release observed in the heterogeneous medium allows for prolonged availability of *p*-AN, which can be therapeutically advantageous.

REFERENCES

1. A. A. Moulay, K. Diaf, Z. Elbahri, A. Mesli, N. Chafi and N. Besbes, *Bull. Chem. Soc. Ethiop.*, **2023**, *37*, 745 (https://doi.org/10.4314/bcse.v37i3.16)
2. A. Rana, M. Adhikary, P. K. Singh, B. C. Das and S. Bhatnagar, *Front. Chem.,* **2023**, *10*, 1095598 (https://doi.org/10.3389/fchem.2022.1095598)
3. R. S. Othman, S. Zarei, H. R. Haghighat, A. Afshar Taromi and H. A. Khonakdar, *Polym. Adv. Technol.*, **2025**, *36*, e70180 (https://doi.org/10.1002/pat.70180)
4. K. Shi, N. Vasconez, S. A. Corcelli and B. D. Smith, *J. Org. Chem.*, **2025**, *90*, 8309 (https://doi.org/10.1021/acs.joc.5c00774)
5. L. P. Hammett, "Physical Organic Chemistry: Reaction Rates, Equilibria and Mechanisms", 2nd edition, McGraw-Hill, Tokyo, Japan, 1970.
6. W. P. Jencks, "General Acid–Base Catalysis of Complex Reactions in Water", in "Progress in Physical Organic Chemistry", S. G. Cohen and A. Streitwieser (Eds.), Interscience, New York, USA, 1964, p. 63 (https://doi.org/ 10.1002/9780470171813.ch2)
7. a) W. P. Jencks, "Catalysis in Chemistry and Enzymology", McGraw-Hill, New York, USA, 1969, p. 490; b) W. P. Jencks, *J. Am. Chem. Soc.*, **1959**, *81*, 475 (https://doi.org/10.1021/ja01511a053)
8. R. W. Layer, *Chem. Rev.*, **1963**, *63*, 489 (https://doi.org/10.1021/cr60225a003)
9. H. Kamogawa, T. Sakai and H. Sohma, *J. Polym. Sci. Part A: Polym. Chem.*, **1988**, *26*, 1335 (https://doi.org/10.1002/pola.1988.080260508)
10. Z. Huang, D. Wan and J. Huang, *Chem. Lett.*, **2001**, *30*, 708 (https://doi.org/10.1246/cl.2001.708)
11. A. Mesli, *Bull. Soc. Chim. Fr.*, **1974**, *9–10*, 2129.
12. A. Mesli, *Bull. Soc. Chim. Fr.*, **1975**, *7–8*, 1745.
13. A. Mesli and J. Tirouflet, *Bull. Soc. Chim. Fr.*, **1975**, *7-8*, 1753.
14. A. Mesli, A. Ali Bey and K. Abdelmezien, *C. R. Acad. Sci. Paris*, 1975, *281*, 385.
15. Z. Bengharez, Z. El Bahri and A. Mesli, *Int. J. Chem. Kinet.*, **2013**, *45*, 404 (https://doi.org/10.1002/kin.20777)
16. A. Mesli, A. Ali Bey and K. Abdelmeziem, *Bull. Soc. Chim. Alg.*, **1975**, *7-8*, 281.
17. A. Ali-Bey, H. F. Loukil, G. Gosselin, A. Mathieu and A. Mesli, *J. Heterocycl. Chem.*, **1982**, *19*, 617 (https://doi.org/10.1002/jhet.5570190333)
18. A. Mesli and J. Tirouflet, *C. R. Acad. Sci. Paris.*, **1968**, *267*, 838.
19. A. Mesli, J. P. Montheard and J. Tirouflet, *C. R. Acad. Sci. Paris.,* **1971**, *272*, 1233.
20. D. Liu, F. Yang, F. Xiong and N. Gu, *Molecules,* **2024**, *29*, 3504 (https://doi.org/10.3390/molecules29153504)
21. A. A. Moulay, N. Chafi, L. Belarbi, Z. Bengharez and A. Mesli, *J. Mater. Environ. Sci.*, **2013**, 4, 474 (https://www.jmaterenvironsci.com/Document/vol4/vol4_N3/59-JMES-297-2012-Moulay.pdf)
22. X. Hu, A. M. Jazani and J. K. Oh, *Polymer*, **2021**, *230*, 124024 (https://doi.org/10.1016/j.polymer.2021.124024)
23. H. Merine, L. Tennouga, A. Mesli, N. Chafi and K. Medjahed, *Am. J. Polym. Sci.*, **2013**, *3*, 99 (http://www.sapub.org/global/showpaperpdf.aspx?doi=10.5923/j.ajps.20130306.01)
24. A. Djouhra, S. Tabti, R. Berenguer, E. Morallón and A. Ourari, *Rev. Roum. Chim.*, **2025**, *70*, 5 (DOI: 10.33224/rrch.2025.70.1-2.01)
25. F. Madani, S. S. Esnaashari, T. J. Webster, M. Khosravani and M. Adabi, *J. Control. Release*, **2022**, *349*, 649 (https://doi.org/10.1016/j.jconrel.2022.07.023)
26. A. T. Qureshi, S. Afrin, S. Asim and M. Rizwan, *Adv. Healthc. Mater.*, **2025**, *14*, e2405260. (https://doi.org/10.1002/adhm.202405260)
27. A. Bouoidina, R. Haldhar, R. Salim, E. Ech-chihbi, H. Ichou, F. El-Hajjaji, B. El Ibrahimi, S. Kaya and M. Taleb, *Korean J. Chem. Eng.*, **2023**, *40*, 235 (https://doi.org/10.1007/s11814-022-1246-5)
28. R. Bera, R. Bandyopadhyay, B. Debnath, G. Dutta and A. Sugumaran, *RSC Adv.*, **2025**, *15*, 23025–23044 (https://doi.org/10.1039/D5RA03188E)
29. T. Fujita, H. Kawashima, E. Sakuradani, T. Sakamoto, A. Ando, J. Ogawa and S. Shimizu, *Biocatal. Agric. Biotechnol.*, **2016**, *8*, 167 (https://doi.org/10.1016/j.bcab.2016.08.011)
30. F. Benachenhou, A. Mesli and R. Guilard, *Arab. J. Chem.*, **2013**, *6*, 313 (https://doi.org/10.1016/j.arabjc.2011.03.007)
31. L. Bélarbi, A. Mesli, , K. Guemra and N. Chafi, *J. Soc. Alger. Chim.*, **1999**, *9*, 203.
32. A. Albert and E. P. Serjeant, "The Determination of Ionization Constants", Chapman & Hall, London, 1971, p. 82.
33. J. Crank, "The Mathematics of Diffusion", 2nd edition, Oxford University Press, Oxford, 1975.
34. T. Higuchi, *J. Pharm. Sci.*, **1963**, *52*, 1145 (https://doi.org/10.1002/jps.2600521210)
35. R. W. Korsmeyer and N. A. Peppas, *J. Control. Rel.*, **1984**, *1,* 89 (https://doi.org/10.1016/0168-3659(84)90001-4)
36. M. Mouffok, I. Abdelmalek, A. Mesli and A. A. Moulay, *Chem. Africa*., **2023**, *6*, 163 (https://dx.doi.org/10.1007/s42250-022-00323-6)
37. M. Mouffok, A. Mesli, I. Abdelmalek and E. Gontier, *J. Serb. Chem. Soc.*, **2016**, *81*, 1183 (https://doi.org/10.2298/JSC160308068M)
38. A. Merdoud, M. Mouffok, A. Mesli, N. Chafi and M. Chaib, *J. Serb. Chem. Soc.*, **2020**, *85*, 531 (https://doi.org/10.2298/JSC190326132M)
39. I. Abdelmalek, M. Mouffok, L. Bennabi and A. Mesli, *Rev. Roum. Chim.*, **2021**, *66*, 1035–1045.